Available online at www.sciencedirect.com

ScienceDirect

Energy Procedia 142 (2017) 1706–1713

Energy Procedia

www.elsevier.com/locate/procedia

9th International Conference on Applied Energy, ICAE2017, 21-24 August 2017, Cardiff, UK

Control algorithm design for degradation mitigation and lifetime improvement of Polymer Electrolyte Membrane Fuel Cells

Pierpaolo Polverino[a,]*, Cesare Pianese[a]

[a]*Department of Industrial Engineering, University of Salerno, via Giovanni Paolo II 132, 84084, Fisciano (SA), ITALY*

Abstract

The improvement of reliability, durability and availability of fuel cell systems represents a key factor for their mass-market deployment in several application areas. The development of advanced algorithms oriented towards fuel cell system monitoring, diagnostics, prognostics and control can significantly reduce the incidence of degradation mechanisms and faulty events on fuel cell performance and durability. Therefore, a valuable increase in system efficiency and lifetime can be achieved by proper design of such algorithms, especially for applications working under highly variable load profiles. The present work deals with the design of a model-based control algorithm aimed at mitigating degradation effects on a Polymer Electrolyte Membrane Fuel Cell (PEMFC) system. Such an algorithm embeds cell degradation models, describing Ostwald ripening and Platinum dissolution mechanisms, which affects the cell Electrochemical Surface Area. The control algorithm is developed aiming at PEMFC durability improvement, while ensuring user power request, and its performance is evaluated in simulated environment addressing stationary power generation applications with variable load profile and comparing the cell degradation decay under different control strategies.

Peer-review under responsibility of the scientific committee of the 9th International Conference on Applied Energy.

Keywords: Polymer Electrolyte Membrane Fuel Cell, Control, Degradation, Lifetime, Mitigation strategies.

1. Introduction

Polymer Electrolyte Membrane Fuel Cells (PEMFCs) are considered one of the most promising power generation systems, based on non-fossil fuels, capable of providing electric power for automotive, portable, backup and remote applications [1]. Nevertheless, their high production costs and reduced durability (with respect to conventional power

* Corresponding author. Tel.: +39-089-96-4178; fax: +39-089-96-4037.
E-mail address: ppolverino@unisa.it

1876-6102
Peer-review under responsibility of the scientific committee of the 9th International Conference on Applied Energy .
10.1016/j.egypro.2017.12.553

systems, such as internal combustion engines) are currently limiting their mass-market deployment. The main causes restraining PEMFC lifetime are substantially related to the several degradation mechanisms the cell is subject to, such as polymer membrane chemical, mechanical and thermal degradation, catalyst dissolution, coarsening and coalescence, carbon corrosion, etc. [2]. Several authors discuss about degradation mitigation, such as Abbou et al. [3], who tested different purging and cooling strategies to reduce cell degradation due to fuel starvation and catalyst loss. Also Jia et al. [4] investigated mitigation strategies to reduce the impact of hydrogen starvation of PEMFCs systems, running under dynamic operation. They observed that starvation could be removed through a two-step startup manoeuver, avoiding detrimental current undershoots. On the same line, Tokarz and Piela [5] investigated the application of a stopping manoeuver to mitigate catalyst degradation when the system is switched off. In the literature review accomplished by Dijoux et al. [6], the authors remarked the importance of performing proper diagnosis in conjunction with control actions that account for the faulty operations. In this way, it is possible to ensure the required performance to the user even if a faulty state is occurring or, as well, degradation phenomena are lowering fuel cell efficiency. According to their findings, many authors discuss about Fault Tolerant Control (FTC), but very few works deal with FTC strategies applications to fuel cell systems.

Therefore, the main contribution of this work, with respect to the current state-of-the-art, consists in the introduction of an innovative control algorithm capable of reducing voltage degradation, and thus increasing fuel cell lifetime, while maintaining the required fuel cell performance (i.e., the user demand is fully satisfied). The algorithm is developed following a model-based design approach by introducing a suitable PEMFC fuel cell model, already presented by the authors [7]. In the following sections, the considered system and control algorithm design is proposed. Afterwards, the control efficacy is evaluated in a simulated environment, to assess the validity of the proposed algorithm.

2. Control algorithm design

2.1. System structure

The system here considered is oriented to stationary power generation applications and is composed by a PEMFC stack and an air blower, which are regulated by means of different controllers. A schematic representation of the accounted components, with related controllers as well as main inputs and outputs is given in Fig. 1. The stack works in open-cathode mode and in dead-end at anode side. Open cathode operation indicates that the air flow fed by the blower provides the stack with the required air amount for the electrochemical reaction and also contributes to stack temperature control. Anode dead-end operation implies that the hydrogen provided to the stack by, e.g., a tank, is totally consumed (i.e. fuel utilization is near 1). Usually, the anode outlet is closed and a purging is performed with a certain frequency, to avoid electrode pressure increase and to remove water surplus. In this work, the dynamic effects induced by the purging are neglected and the hydrogen is considered instantaneously fed by an infinite capacity tank.

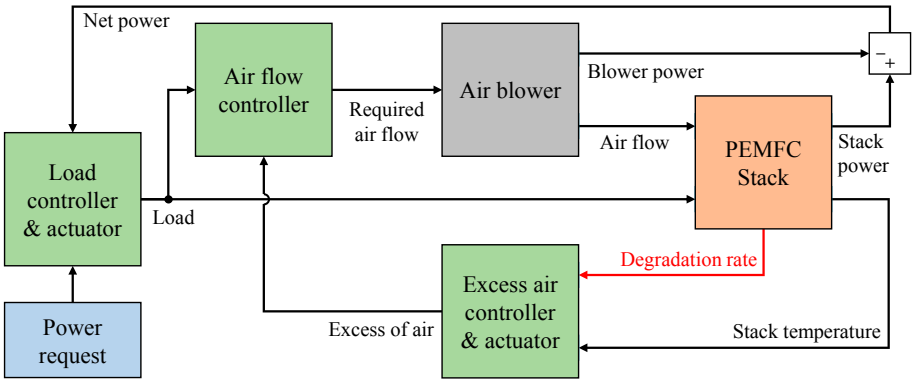

Fig. 1. Schematic representation of system components, controllers and main inputs/outputs.

The user request is represented by a variable power demand, which includes also the power electronics needed for the stack/user interfacing. The current (i.e., load) to be drawn from the stack is evaluated through a feedback control based on user power request, whereas the required air flow from the blower is controlled by means of a feedforward algorithm. Moreover, the stack temperature is regulated through a feedback control logic, acting on the excess of air as adaptable parameter. In all cases, an actuation delay is introduced to distinguish between the defined set-points and the current inputs sent to the specific component.

2.2. PEMFC stack and air blower models

The stack voltage V_{fc} is represented through the model described in [7]. This model provides a cell voltage equation that embeds cell degradation related to the combination of Ostwald ripening and Platinum dissolution (affecting fuel cell Electrochemical Surface Area – ECSA). The stack voltage model can be resumed through the following expression:

$$V_{fc} = f\left(I, T_{fc}, p_{H_2}, p_{O_2}, t\right) \tag{1}$$

which highlights voltage dependence upon operating parameters (i.e., current I, temperature T_{fc} and reactants partial pressures p_{H2} and p_{O2}) and time (due to degradation). The stack outlet temperature T_{fc} is computed by means of a simple energy balance equation, defined through a Mean Value Modelling (MVM) approach:

$$K_{fc}\frac{dT_{fc}}{dt} = \dot{E}_{in}\left(T_{in}\right) - \dot{E}_{out}\left(T_{fc}\right) - V_{fc}I \tag{2}$$

where the term K_{fc} is the stack heat capacity, $\dot{E}_{in}$ and $\dot{E}_{out}$ are the inlet and outlet energy flows, function of the inlet and outlet temperatures, respectively. Assuming that the inlet and outlet energy flows can be expressed as follows:

$$\dot{E}_{in} = \dot{m}_{air}c_{p_{air}}T_{b,out} + \frac{I}{2F}N_{fc}\left(M_{H_2}c_{p_{H_2}}T_{H_2,in} + LHV_{H_2}\right) \tag{3}$$

$$\dot{E}_{out} = \left(\dot{m}_{air} - \frac{I}{4F}N_{fc}M_{air}\right)c_{p_{air}}T_{fc} + \frac{I}{2F}N_{fc}c_{p_{H_2O}}M_{H_2O}T_{fc} \tag{4}$$

the energy balance of equation (2) can be further presented as:

$$K_{fc}\frac{dT_{fc}}{dt} = \dot{m}_{air}c_{p_{air}}\left(T_{b,out} - T_{fc}\right) + \frac{I}{2F}N_{fc}\left(M_{H_2}c_{p_{H_2}}T_{H_2,in} + LHV_{H_2} + \frac{c_{p_{air}}}{2}M_{air}T_{fc} - c_{p_{H_2O}}M_{H_2O}T_{fc}\right) - V_{fc}I \tag{5}$$

where $\dot{m}_{air}$ and $T_{b,out}$ are the air blower outlet mass flow and temperature, respectively, F is the Faraday's constant, N_{fc} is the number of cells, LHV_{H2} is the hydrogen Lower Heating Value and $T_{H2,in}$ is the hydrogen tank outlet temperature. The parameters c_{pair}, c_{pH2} and c_{pH2O} as well as M_{air}, M_{H2} and M_{H2O} are the specific heat capacities c_p and molar masses M of air hydrogen and water, respectively.

The air blower provides the air flow amount needed by the stack $\dot{m}_{air}$, in accordance with the desired set-point $\dot{m}_{air,set}$. The blower actuation is represented through a first order response:

$$\frac{d\dot{m}_{air}}{dt} = \frac{\dot{m}_{air,set} - \dot{m}_{air}}{\tau_b} \tag{6}$$

with a specific time constant τ_b. This response represents the actuation delay related to the electric motor powering the blower, which is controlled so as to regulate the air mass flow. The blower output temperature $T_{b,out}$ and absorbed power P_b are expressed with equations (7) and (8), respectively:

$$T_{b,out} = T_{b,in}\beta^{\frac{k-1}{k}} \tag{7}$$

$$P_b = \dot{m}_{air}\frac{c_{p_{air}}}{\eta_b}\left(T_{b,out} - T_{b,in}\right) \tag{8}$$

where $T_{b,in}$ is the inlet blower temperature, β is the blower pressure ratio, k is the polytropic index and η_b is the blower efficiency. The net power P_{net} provided to the user is evaluated as:

$$P_{net} = V_{fc}I - P_b \tag{9}$$

2.3. Standard controllers

The current set-point I_{set} to be drawn from the stack is regulated through a feedback Proportional-Integral (PI) controller, based on the difference between the user power demand P_{des} and the provided net power (equation (9)). On the same line, the stack temperature is controlled through a feedback PI controller (equation (11)) by varying the excess of air set-point value $\zeta_{air,set}$, to keep the temperature nearby the desired set-point T_{set}.

$$I_{set} = I + K_P^{cur}\left(P_{des} - P_{net}\right) + K_I^{cur}\int\left(P_{des} - P_{net}\right)dt \tag{10}$$

$$\zeta_{air,set}^{temp} = \zeta_{air} + K_P^{temp}\left(T_{fc} - T_{set}\right) + K_I^{temp}\int\left(T_{fc} - T_{set}\right)dt \tag{11}$$

In the previous equations, the terms K_P and K_I are the proportional and integral controller coefficients, designed according to the Zigler-Nickols approach [8]. The actuation delay of the current I is modelled by means of a first order response (as done in equation (6)) with a related time constant τ_{cur}. The air blower flow is instead regulated through a feedforward controller, which outlines the desired air flow $\dot{m}_{air,set}$ upon the knowledge of current and excess of air set-points:

$$\dot{m}_{air,set} = \frac{I_{set}}{4F}M_{air}N_{fc}\zeta_{air,set}^{temp} \tag{12}$$

Through the current air flow actuated by the blower (see equation (6)), the current excess of air (to be fed to equation (11)) can be estimated:

$$\zeta_{air} = \frac{4F}{M_{air}N_{fc}}\frac{\dot{m}_{air}}{I} \tag{13}$$

2.4. Degradation control algorithm

The main novelty of this work consists in the implementation of a Proportional (P) controller, which acts on the excess of air (as the temperature controller) in order to reduce stack degradation. This strategy is developed upon the estimation of ECSA degradation rate v performed by means of the degradation model presented in [7]. This rate is

evaluated as a discrete derivative of ECSA time behavior over a fixed time window Δt (equation (13)), and the excess of air correction is performed as shown in equation (14). Also in this case, the excess of air set-point influences the air flow through equation (12).

$$\nu(t) = -\frac{ECSA(t) - ECSA(t-\Delta t)}{\Delta t} \tag{14}$$

$$\zeta_{air,set}^{ecsa} = \zeta_{air} + K_P^{ecsa}\left[\nu(t+\Delta t) - \nu(t)\right] \tag{15}$$

3. Results and discussion

The efficacy of the proposed control algorithm is investigated by evaluating system performance and degradation with respect to different control strategies. A simulation analysis is performed and the values considered for all the introduced parameters are proposed in Table 1.

Table 1. Simulation parameters used for the control strategies analysis; voltage and electrochemical model references can be found in [7].

Parameter	Description	Unit	Value
β	Air blower pressure ratio	[-]	1.2
$c_{p_{air}}$	Air specific heat capacity	[J kg^{-1} K^{-1}]	1012
$c_{p_{H_2}}$	Hydrogen specific heat capacity	[J kg^{-1} K^{-1}]	14549.5
$c_{p_{H_2O}}$	Vapor specific heat capacity	[J kg^{-1} K^{-1}]	2001.5
η_b	Air blower efficiency	[-]	0.4
F	Faraday's constant	[C mol^{-1}]	96485
K_{fc}	Stack heat capacity	[J K^{-1}]	200
K_I^{cur}	Current controller Integral coefficient	[A J^{-1}]	10^{-4}
K_I^{temp}	Current controller Integral coefficient	[K^{-1} s^{-1}]	10^{-7}
K_P^{cur}	Current controller Integral coefficient	[A W^{-1}]	10^{-2}
K_P^{ecsa}	Current controller Integral coefficient	[s m^{-2}]	10^{6}
K_P^{temp}	Current controller Integral coefficient	[K^{-1}]	10^{-3}
k	Polytropic constant	[-]	1.4
LHV_{H_2}	Hydrogen Lower Heating Value	[J mol^{-1}]	241827
M_{air}	Air molar mass	[g mol^{-1}]	28.84
M_{H_2}	Hydrogen molar mass	[g mol^{-1}]	2
M_{H_2O}	Vapor molar mass	[g mol^{-1}]	18
N_{fc}	Number of cells	[-]	50
p_{H_2}	Hydrogen partial pressure	[bar]	1.14
T_{set}	Stack temperature set-point	[°C]	45
τ_b	Blower actuation characteristic time	[s]	5
τ_{cur}	Current actuation characteristic time	[s]	0.1

The user power request is assumed being a variable profile (sketched as a solid blue line in Fig. 2a), which varies randomly between 1 kW and 3 kW over 24 h with a time step of 30 min. Three different control strategies are evaluated:

- Control Strategy 1 (CS1): this strategy aims at controlling only the temperature and the excess of air set-point is defined through equation (11);
- Control Strategy 2 (CS2): this strategy aims at controlling only the stack degradation and the excess of air set-point is defined through equation (14);
- Control Strategy 3 (CS3): this strategy combines both temperature and degradation control and the excess of air is defined through superposition (i.e., summation) of the two set-points defined in equations (11) and (14).

For any considered control strategy, the net power perfectly matches the user request (see dashed red line in Fig. 2a). This result ensures that the user request is always met, with only a slight change in the single cell voltage behavior at different control strategies (Fig. 2b). A substantial change is observed instead for the temperature (Fig. 2c), due to the completely different strategies. The results in terms of maximum, mean and minimum stack temperature, with corresponding standard deviation, fulfilled over the time observation of 24 h are resumed in Table 2, in addition to the information of the achieved ECSA, normalized with respect to its initial condition (i.e., ECSA @ 0 h).

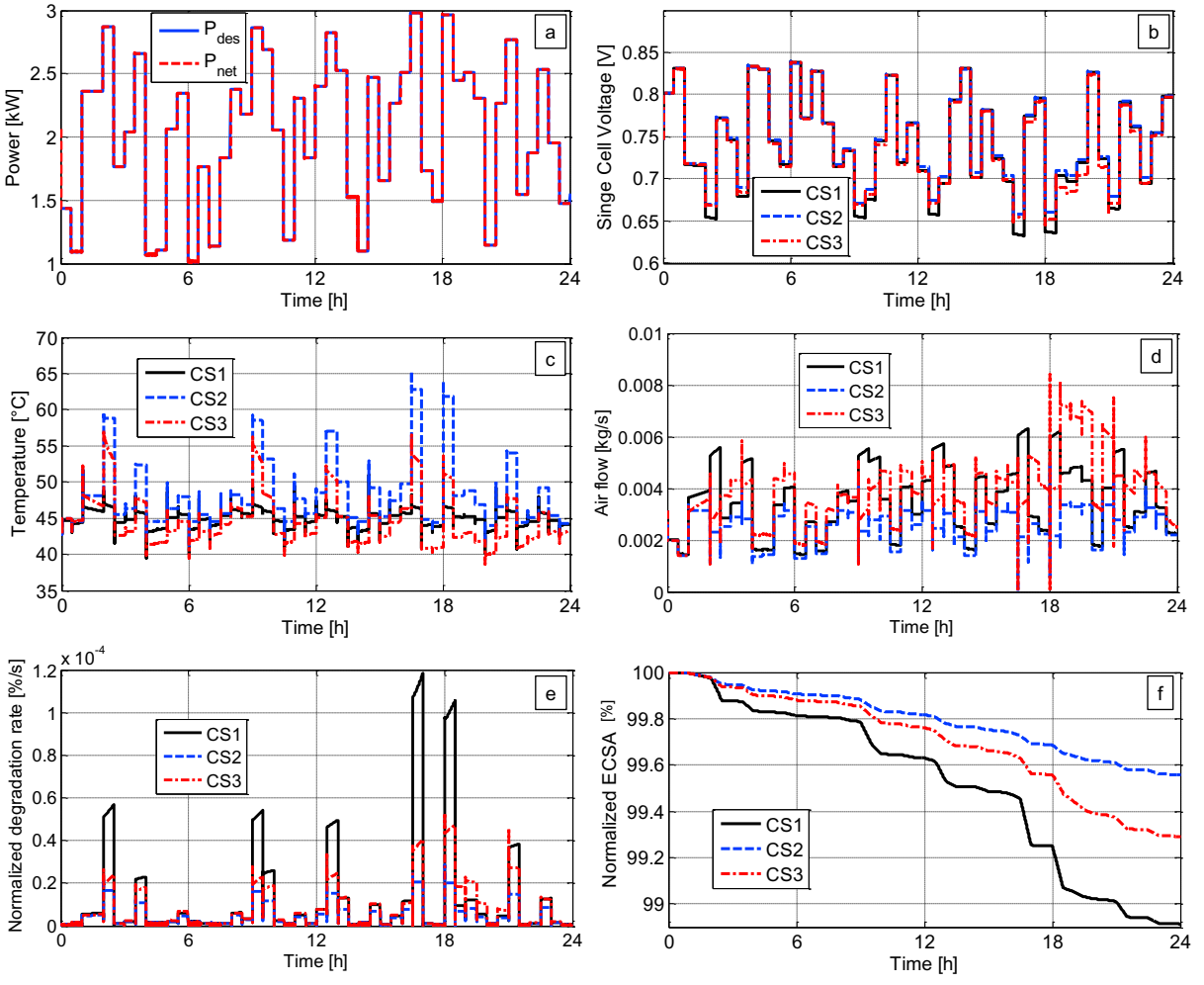

Fig. 2. Results obtained for the same user power request profile (a) in terms of voltage (b), temperature (c), air flow (d), normalized degradation rate (e) and normalized ECSA (f) time behaviors for different control strategies (CS1: only temperature control; CS2: only degradation control; CS3: combined control of temperature and degradation).

The control strategy CS1 is designed to keep the stack temperature close to the defined set-point (here assumed being 45°C). In this case, the temperature slightly oscillates around such value, as visible from the solid black line in Fig. 2c and from the mean temperature reported in Table 2. Indeed, such temperature differs from the set-point of about -0.2% with a small dispersion, as proved by the standard deviation of 1.04°C. The resulting air flow rate is represented in Fig. 2d, showing an almost regular behavior over the observed time window. In Fig. 2e is instead represented the degradation rate normalized with respect to the ECSA initial state. The application of such strategy induces a high fluctuation of the degradation rate, with a maximum value of about $1.2 \cdot 10^{-4}$ %/s at the maximum load request. The resulting ECSA reduction over 24 h is then -1.087%, as also observable from the behavior shown in Fig. 2f. It is worth noting that, as expected, the slope is greater at high degradation rates.

Table 2. Result after 24 h of operation.

Control Strategy	T_{fc} max [°C]	T_{fc} mean [°C]	T_{fc} min [°C]	T_{fc} standard dev. [°C]	Normalized *ECSA* @ 24 h [%]
CS1	52.3	44.9	39.4	1.04	98.913
CS2	65.3	47.9	41.2	4.60	99.558
CS3	57.2	44.5	38.6	3.40	99.292

The second strategy CS2 do not account for any temperature control, but aims at reducing as much as possible the ECSA degradation. The resulting effect consists in the uncontrolled increase in the stack temperature at high load (i.e., power), with temperature peaks of 65°C and a standard deviation of 4.6°C. This strong oscillation is a consequence of the smaller air flow rate, as visible from the dashed blue line in Fig. 2d. However, the degradation rate over 24 h is much lower compared to that of strategy CS1 (see Fig. 2e). Indeed, in this case the achieved ECSA reduction corresponds to -0.442%, with a decrease in the normalized degradation rate of about -59%. However, the average stack temperature deviates from the set-point of more than +6%, with a greater dispersion (indeed, the achieved maximum temperature is 25% higher than that of the previous strategy). Although effective in reducing degradation, such strategy do not allow proper temperature control, which may induce other detrimental mechanisms to take place (e.g., membrane dehydration, mechanical stresses, etc.), and should not be applied on real systems.

A good compromise can be found in the application of control strategy CS3, where both information on temperature set-point and ECSA degradation rate are accounted. In this case, the average stack temperature deviates of about -1% from the set-point, with maximum and minimum values near those achieved with CS1 (see Table 2). What is interesting to note is that the ECSA degradation over 24 h is now -0.708%, with a reduction of about -35% in the normalized degradation rate. A further comment can be done on the air flow rate (dot-dashed red line in Fig. 2d), which assumes an irregular behavior over the time window. This effect can be due to the interaction between the different requirements (i.e., temperature and degradation regulations), which induces the air flow to abruptly increase around 18 h. Such deviation could be related to the compensation of a strong temperature fluctuation, that would have occurred under uncontrolled temperature strategy (dashed blue line in Fig. 2c). Afterwards, the integral characteristic of the temperature controller slowly bring the stack temperature closer to the set-point, with an evident monotonous overall reduction in the air flow rate. Nevertheless, such event do not affect the power production of the system, which suitably respect the user requests.

4. Conclusions

The work described in this paper proposed a model-based control algorithm capable of reducing fuel cell degradation rate under variable load profile. The system under study is a PEMFC-based power generation unit aimed at stationary power generation applications. The target power is assumed ranging between 1 kW and 3 kW over 24 h, with a time step of about 30 min. The system is controlled by means of two feedback PI controllers, one defining the current set-point, to meet the required power, and the other to evaluate the excess of air set-points, to control stack temperature. Moreover, a feedforward controller is introduced to define air blower mass flow set-point.

The innovation of the paper consisted in the introduction of a further model-based controller, which defines excess of air set-point based on estimated ECSA degradation rate. The controller is evaluated in a simulated environment

comparing three different control strategies, one with only temperature control (CS1), one with only degradation control (CS2) and one with both temperature and degradation control (CS3). The achieved results proved that the introduction of the degradation based control algorithm substantially improves PEMFC durability. Nevertheless, removing temperature control led to dangerous temperature peaks, which could enhance other faults and degradation mechanisms (e.g., membrane drying, thermal stresses, etc.) and reduce in turn fuel cell lifetime. Therefore, the combination of both controllers (i.e., control strategy CS3) gives the best trade-off between degradation rate and temperature control, with an overall decrease of 35% in the ECSA over 24 h with respect to CS1.

Future works will entail the introduction of a more complex fuel cell model, so as to account for more detailed components and phenomena interaction. Moreover, the assessment of other operating conditions and applications will be also considered, to evaluate controller performance in different environments.

Acknowledgements

This research has been funded by the Italian Government, with the PON project “Fuel Cell Lab – Innovative systems and high efficient technologies for polygeneration (PON03PE_00109/1).

References

[1] Larminie J, Dicks A. Fuel Cell Systems Explained. John Wiley & Sons Ltd; 2003.
[2] Jahnke T, Futter G, Latz A, Malkow T, Papakonstantinou G, Tsotridis G, et al. Performance and degradation of Proton Exchange Membrane Fuel Cells: State of the art in modeling from atomistic to system scale. Journal of Power Sources; 304; 2016. p. 207-233.
[3] Abbou S, Dillet J, Maranzana G, Didierjean S, Lottin. Local potential evolutions during proton exchange membrane fuel cell operation with dead-ended anode - Part II: Aging mitigation strategies based on water management and nitrogen crossover. Journal of Power Sources; 340; 2017. P. 419-427.
[4] Jia F, Guo L, Liu H. Mitigation strategies for hydrogen starvation under dynamic loading in proton exchange membrane fuel cells. Energy Conversion and Management; 139; 2017. p. 175-181.
[5] Tokarz W, Piela P. Mitigation of catalysts degradation upon stopping work of polymer electrolyte membrane fuel cells for longer time. International Journal of Hydrogen Energy; 41; 2016. p. 15002-15006.
[6] Dijoux E, Yousfi-Steiner N, Benne M, Péra MC, Perez BG. A review of fault tolerant control strategies applied to proton exchange membrane fuel cell systems. Journal of Power Sources; 359; 2017. p. 119-133.
[7] Polverino P, Pianese C. Model-based prognostic algorithm for online RUL estimation of PEMFCs. Proceedings of the 3rd Conference on Control and Fault-Tolerant Systems, SysTol16; 2016. p. 599-604.
[8] Ziegler JG, Nichols NB. Optimum settings for automatic controllers. Transactions of the ASME; 64; 1942. p. 759–768.